

## Electrochemical removal of carbamazepine in water with Ti/PbO<sub>2</sub> cylindrical mesh anode

J. D. García-Espinoza, P. Gortáres-Moroyoqui, M. T. Orta-Ledesma, P. Drogui and P. Mijaylova-Nacheva

### ABSTRACT

Carbamazepine (CBZ) is one of the most frequently detected organic compounds in the aquatic environment. Due to its bio-persistence and toxicity for humans and the environment its removal has become an important issue. The performance of the electrochemical oxidation process and *in situ* production of reactive oxygen species (ROS), such as O<sub>3</sub> and H<sub>2</sub>O<sub>2</sub>, for CBZ removal have been studied using Ti/PbO<sub>2</sub> cylindrical mesh anode in the presence of Na<sub>2</sub>SO<sub>4</sub> as supporting electrolyte in a batch electrochemical reactor. In this integrated process, direct oxidation at anode and indirect oxidation by *in situ* electrogenerated ROS can occur simultaneously. The effect of several factors such as electrolysis time, current intensity, initial pH and oxygen flux was investigated by means of an experimental design methodology, using a 2<sup>4</sup> factorial matrix. CBZ removal of 83.93% was obtained and the most influential parameters turned out to be electrolysis time, current intensity and oxygen flux. Later, the optimal experimental values for CBZ degradation were obtained by means of a central composite design. The best operating conditions, analyzed by Design Expert<sup>®</sup> software, are the following: 110 min of electrolysis at 3.0 A, pH = 7.05 and 2.8 L O<sub>2</sub>/min. Under these optimal conditions, the model prediction (82.44%) fits very well with the experimental response (83.90 ± 0.8%). Furthermore, chemical oxygen demand decrease was quantified. Our results illustrated significant removal efficiency for the CBZ in optimized condition with second order kinetic reaction.

**Key words** | carbamazepine, electrooxidation, hydrogen peroxide, reactive oxygen species

**J. D. García-Espinoza** (corresponding author)  
Facultad de Ingeniería,  
Universidad Nacional Autónoma de México  
(UNAM),  
Paseo Cuauhnáhuac 8532, Col. Progreso,  
Jiutepec, Morelos 62550,  
Mexico  
E-mail: [jgarciaespinoza@gmail.com](mailto:jgarciaespinoza@gmail.com)

**P. Gortáres-Moroyoqui**  
Departamento de Biotecnología y Ciencias  
Alimentarias,  
Instituto Tecnológico de Sonora (ITSON),  
5 de Febrero 818 Sur C.P.,  
Cuidad Obregón, Sonora 85000,  
Mexico

**M. T. Orta-Ledesma**  
Instituto de Ingeniería,  
UNAM. Ciudad Universitaria,  
Coyoacán, D.F. 04510,  
Mexico

**P. Drogui**  
Institut national de la recherche scientifique  
(INRS-Eau Terre et Environnement),  
8 Université du Québec,  
490 rue de la Couronne, Québec,  
QC G1K 9A9 Canada

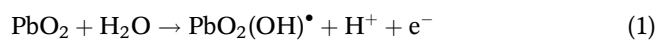
**P. Mijaylova-Nacheva**  
Instituto Mexicano de Tecnología del Agua (IMTA),  
Paseo Cuauhnáhuac 8532, Col. Progreso,  
Jiutepec, Morelos 62550,  
Mexico

### INTRODUCTION

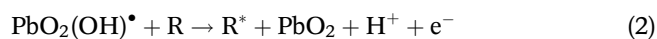
An increasing amount of pharmaceuticals are consumed for the prevention, diagnosis and treatment of illness in humans and animals. The worldwide average per capita consumption of pharmaceuticals per year is estimated to be about 15 g and in the industrialized countries the value is expected to be 50 g (Zhang *et al.* 2008). The occurrence of pharmaceutically active compounds in water bodies, which are not completely removed by conventional treatment processes, is an emerging issue. Carbamazepine (CBZ) is one of the most detected pharmaceuticals in the environment, due to its continuous input and persistence in the environment even at low concentrations (µg/L or ng/L) (Miao *et al.* 2005). This compound is an established drug to treat different psychiatric disorders such as psychomotor epilepsy and it is also effective

in the treatment of trigeminal neuralgia (Daghrir *et al.* 2013; Mohapatra *et al.* 2014a). The worldwide CBZ consumption is estimated to be 1,014 ton per year (Zhang *et al.* 2008). Removal of CBZ during biological wastewater treatment was found to be less than 10%, sorption in the secondary sludge was insignificant and photodegradation requires more than 100 days (Chenxi *et al.* 2008; Al Aukidy *et al.* 2012). Therefore, it is important to develop more efficient processes with the purpose of accomplishing the CBZ degradation either to less harmful compounds or to achieve its mineralization. Advanced oxidation processes may represent an alternative for a complete degradation of organic trace pollutants. These processes can be broadly defined as aqueous phase oxidation methods based on the intermediacy

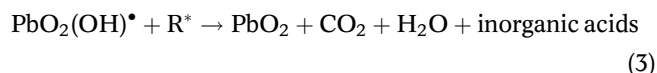
of highly reactive species such as hydroxyl radicals ( $\text{OH}^\bullet$ ) (activation energy,  $E^\circ$ , of  $(\text{OH}^\bullet/\text{H}_2\text{O}) = 2.8 \text{ V}$ ),  $\text{O}_2^{\bullet-}$  and  $\text{HO}_2^\bullet$  in the mechanisms leading to the destruction of the target pollutant until total mineralization is reached (Comninellis *et al.* 2008). Advanced treatment technologies, such as photocatalysis (Mohapatra *et al.* 2014b), photoelectrocatalysis (Daghrir *et al.* 2013), ozonation (Palo *et al.* 2012), sonochemical degradation (Tran *et al.* 2013) and Fenton oxidation (Monsalvo *et al.* 2015), were effective in removing CBZ; however, large chemical consumption of  $\text{H}_2\text{O}_2$  or  $\text{O}_3$  and the relatively high treatment costs constitute major barriers for large-scale applications. The electrochemical oxidation process has been proved to be a successful option for the removal of recalcitrant compounds. In the electrochemical oxidation process exist two types of oxidation: indirect and direct. The latter may be achieved through mineralization with hydroxide radical ( $\text{OH}^\bullet$ ) produced by dimensionally stable anodes having high oxygen overvoltage, such as  $\text{SnO}_2$  or  $\text{PbO}_2$  (Tran *et al.* 2009). It is found that the prerequisite for anodic reactions is the anodic discharge of  $\text{H}_2\text{O}$  at  $\text{PbO}_2$  surface to produce adsorbed hydroxyl radicals (Dai *et al.* 2014), which can be presented by reaction (1).



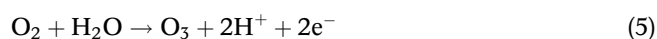
The next step is the oxidation of the organic compounds (R) owing to their interaction with ( $\text{OH}^\bullet$ ) (reaction (2)).  $\text{R}^*$  represents the oxidized organic compound.



Finally, the electrogenerated ( $\text{OH}^\bullet$ ) in the  $\text{PbO}_2$  can achieve the complete degradation of the organic compounds according to reaction (3).



On the other hand, indirect oxidation may be accomplished through electrochemical generation of a mediator in solution, such as  $\text{HClO}$ ,  $\text{HBrO}$  or  $\text{H}_2\text{S}_2\text{O}_8$ . Furthermore, reactive oxygen species (ROS) such as hydrogen peroxide ( $\text{H}_2\text{O}_2$ ) or ozone ( $\text{O}_3$ ) may be produced *in situ* in aqueous medium by reducing dissolved molecular oxygen with  $2\text{e}^-$  at the cathode surface (reaction (4)) (Wu *et al.* 2012) or reacting at the anode (reaction (5)), respectively.



It is important to note that this way of ROS production is a sustainable process since it does not use toxic solvents and the species are continuously generated, eliminating in this way the transportation costs and handling risks (Peralta *et al.* 2013). Furthermore,  $\text{H}_2\text{O}_2$  and  $\text{O}_3$  are readily soluble in water and nontoxic; also they exhibit high oxidative power and capability to oxidize recalcitrant compounds to less harmful products in solutions with  $E^\circ$  (V) of 1.77 and 2.08, respectively. That is why the organic compound degradation could be increased by the combination of electrochemical oxidation and electrogenerated ROS oxidation. The performance of this integrated process has been investigated in previous works (Shen *et al.* 2005; Zhu *et al.* 2014); nevertheless, there does not exist a previous study of electrolysis time, current intensity, initial pH and the presence of oxygen, by means of an experimental design methodology, in the removal of the recalcitrant compound CBZ. The aim of this study was to evaluate the performance of electrooxidation and *in situ* ROS production in an integrated process of simultaneous direct and indirect oxidation for CBZ removal, using  $\text{Ti}/\text{PbO}_2$  anode and Ti cathodes.

## MATERIALS AND METHODS

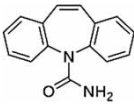
### Preparation of the synthetic solution

CBZ analytical grade reagent was obtained from Sigma-Aldrich. Stock solution was prepared in an amber flask by dissolving 0.2 g of CBZ in 10 mL of methanol. The physico-chemical properties of the compound are summarized in Table 1. This solution was kept in a refrigerator ( $3^\circ\text{C}$ ). Later, 0.5 mL of the stock solution was mixed in 1 L of distilled water using a magnetic stirrer for 15 min. The resulting synthetic solution presented a CBZ concentration of 10 mg/L and chemical oxygen demand (COD) of 600 mg  $\text{O}_2/\text{L}$ . The conductivity of the solution was increased using  $\text{Na}_2\text{SO}_4$  as supporting electrolyte at a concentration of 1 g/L.  $\text{Na}_2\text{SO}_4$  was an analytical grade reagent supplied by J. T. Baker.

### Electrolytic reactor set-up

The experimental set-up was constituted of a 1.5 L electrochemical reactor made of acrylic material, a centrifugal pump, a power supply with a maximum current of 15 A

**Table 1** | Physico-chemical properties of CBZ

Molecular formula	Chemical structure	Molecular weight (g/mol)	Solubility (mg/L)	pK <sub>a</sub>	LogK <sub>ow</sub>
C <sub>5</sub> H <sub>12</sub> N <sub>2</sub> O		236.1	17.7 <sup>a</sup>	13.9 <sup>b</sup>	2.45 <sup>a</sup>

<sup>a</sup>Zhang *et al.* (2008).<sup>b</sup>Chenxi *et al.* (2008).pK<sub>a</sub>: acid dissociation constant; logK<sub>ow</sub>: octanol–water partition coefficient.

at a potential of 40 V (Sorensen DLM 40-15) and an oxygen concentrator (AEROUS, Clean Water Tech) (Figure 1). Inside the reactor, three cylindrical mesh electrodes, two cathodes (Ti) and an anode (Ti/PbO<sub>2</sub>) were installed with an inter-electrode gap of 0.5 cm. The anode, collocated between the cathodes, had an active surface of 207 cm<sup>2</sup>. The total surface area of cathodes was 430 cm<sup>2</sup>. Pure oxygen was injected in the bottom of the reactor. Water recirculation was preferred as a mass transfer process promoter over a magnetic stirrer due to the reactor design, where the oxygen inlet was in the bottom. The recirculation was performed using a peristaltic pump operated at a constant flow of 1,700 mL/min, providing a high turbulence (Reynolds number of 5,000) and high mass transfer coefficient ( $63 \times 10^{-3}$  cm/min) in the reactor. All the experiments were performed at room temperature of 20 °C, under galvanostatic conditions using 1 L of synthetic solution. After each experiment, electrodes were introduced into nitric acid solution (5% vol.) for 5 min in order to avoid any fouling.

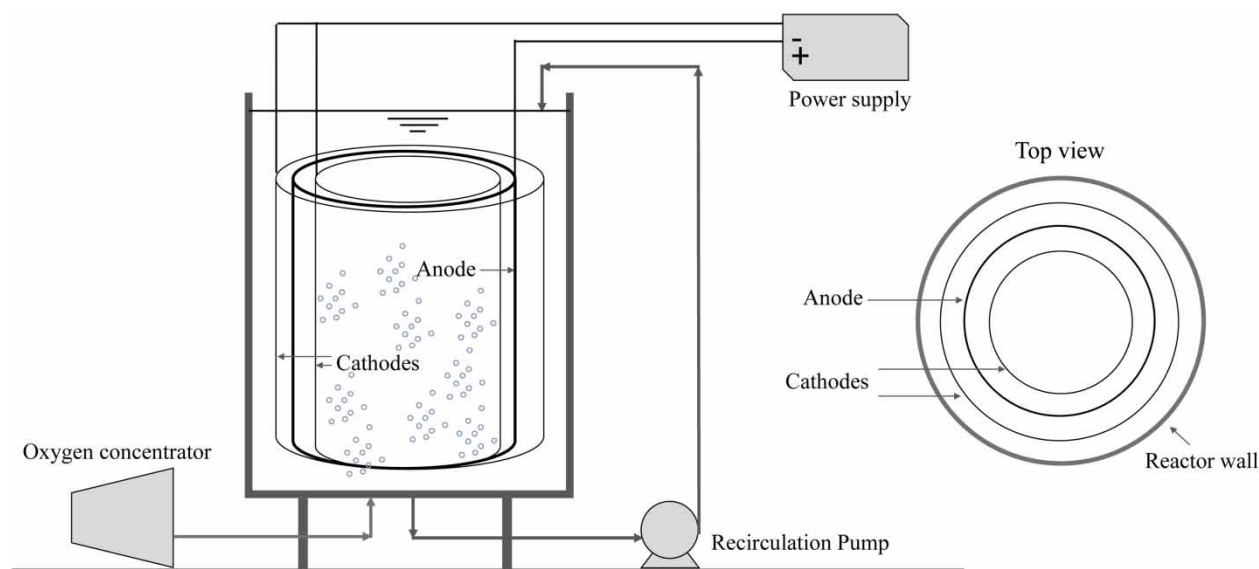
## Analytical details

### CBZ and COD measurement

The concentration of initial and residual CBZ was determined by UV absorption spectral measurements method at 285 nm using spectrophotometry (Cary 60 UV-Vis, Agilent Technologies). A calibration curve of known CBZ concentration (0.0–12.0 mg/L) versus absorbance value was used to determine the residual CBZ concentration and to define the removal efficiency. COD was determined by means of the Hach method.

### Oxidant agent measurements

The oxidant production was estimated using the Wessler reaction, which oxidizes iodide ions into iodine. When oxidant agents are present in solution, iodide ions are oxidized to give iodine. When excess I<sup>-</sup> ions are present in the solution, I<sub>2</sub> reacts with the excess of I<sup>-</sup> to form the I<sub>3</sub><sup>-</sup> ion

**Figure 1** | Schematic diagram of the experimental set-up.

according to reaction (6).



Tri-iodide was analyzed by absorbance measurements using a spectrophotometer at 352 nm. The total oxidants concentration was determined by means of the Beer-Lambert law (molar absorption coefficient = 26,303 L/mol cm) (Tran & Drogui 2013).

### Experimental procedure

The traditional one-factor-at-a-time approach has been widely used to optimize the effects of various factors in a process. Nevertheless, this approach is a time-consuming method and fails to consider any possible interaction between the factors (Wu *et al.* 2012). To solve these problems, response surface methodology (RSM) is proposed. RSM is a collection of mathematical and statistical techniques that are useful for the modelling and for analysis of problems in which a response of interest is influenced by several variables and the objective is to optimize this response (Montgomery 2008; Wu *et al.* 2012). A set of preliminary assays was first carried out in order to determine the effect of current intensity, time and oxygen flux in CBZ removal and its experimental range. Later, a factorial design (FD) was used to investigate the effect of the factors and their interactions. The pH values of pharmaceutical industry effluents have a high fluctuation, usually from 4 to 8; therefore the pH effect was not evaluated in preliminary experiments and all the pH range was considered in the FD. Afterwards, a central composite design (CCD) was employed to optimize the process and the pH range was extended from 2 to 10 in this CCD. Once the optimal conditions had been determined, a final set of experiments was performed in order to confirm the model reproducibility. Four independent factors were studied: time, current intensity, initial pH and oxygen flux. A, FD and a CCD with six replicates in the center led to a total of 30 experiments. CBZ and COD removal were considered as the response. Experimental data were analyzed using Design Expert<sup>®</sup> program software (Design Expert 7, Stat-Ease Inc., Minneapolis). RSM has been applied for the removal of recalcitrant organic compounds in water. For instance, Jiang *et al.* (2013) evaluated the effect of the concentration of hollow glass microspheres coated with TiO<sub>2</sub>, the concentration of terephthalic acid and irradiation time in dimethyl phthalate photocatalytic degradation. The optimum conditions for (OH)<sup>·</sup> generation were 8.0 g/L of photocatalyst, 4.0 mM of acid and 20 min of irradiation. Under those

conditions, pollutant was readily degraded in correlation with the (OH)<sup>·</sup> produced.

## RESULTS AND DISCUSSION

### Preliminary experiments

The first set of experiments was conducted to determine the CBZ removal at different current intensities: 0.5, 1.0, 2.0, 3.0 and 5.0 A (current densities of 2.41, 4.84, 9.66, 14.50 and 24.15 mA/cm<sup>2</sup>, respectively) for a treatment time of 120 min. Recycling flow rate of 1,700 mL/min, 1 g/L of Na<sub>2</sub>SO<sub>4</sub> and initial CBZ concentration of 10 mg/L at neutral pH were the conditions in the assays. Figure 2 shows the results of CBZ removal at different current intensities. Effectiveness of CBZ oxidation increased with current intensity until 3.0 A and remained the same at 5.0 A. This behavior indicates that the highest (OH)<sup>·</sup> production was at 3.0 A; when this value increased, secondary parasitic reactions were induced and the efficiency was diminished. At 0.5 A, the CBZ removal was low (only 55%).

In order to determine the total oxidants production, experiments of 60 min, using 1 g/L of Na<sub>2</sub>SO<sub>4</sub> at 3.0 A were performed with and without oxygen in absence of CBZ and methanol. The addition of pure oxygen enhanced the oxidant production from 0.007 mmol/L (without oxygen addition) to 0.024, 0.030 and 0.050 mmol/L at 0.5, 1.5 and 3.0 L/min, respectively (Figure 3). Taking into account

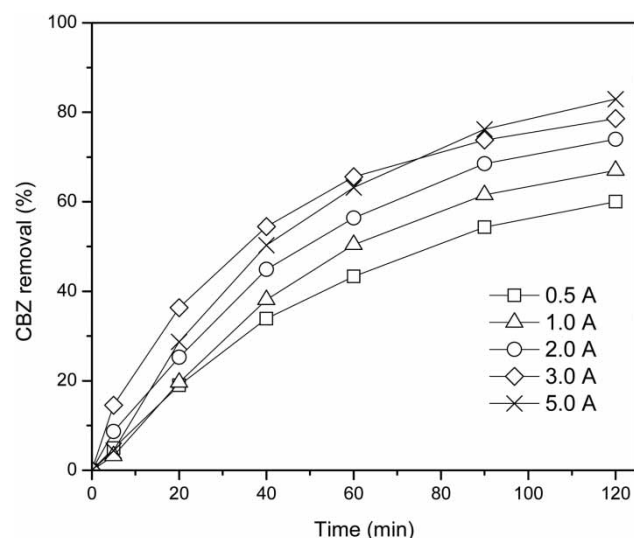


Figure 2 | Preliminary electrooxidation assays for CBZ removal at different current intensities.

the high reactivity and short half-life (approximately  $10^{-9}$  s) of the ROS ( $O_2^-$ ,  $HO_2$ ,  $(OH)^\cdot$ , etc.) the increase in oxidant production is determined as the presence of ROS such as  $H_2O_2$  and  $O_3$ . It seems that there is a relation between the ROS production and oxygen flux. When the dissolved oxygen in the solution increases, higher amounts of  $O_2$  interact at the electrode's surface resulting in ROS generation. The most popular cathode material for  $H_2O_2$  electrogeneration are those made of carbon such as graphite or vitreous carbon (Khataee *et al.* 2011; Guitaya *et al.* 2014; Zhu *et al.* 2014). This material is effective due to its high surface area. Nevertheless, successful  $H_2O_2$  production using Ti mesh electrodes has been reported (Yang *et al.* 2007). These studies agree that at higher active surface area, the  $H_2O_2$  production is higher. In our case, 430  $cm^2$  Ti cathode surface area was used.

Without oxygen addition, oxidants were generated because of the presence of sulfate ions in the solution, which were oxidized, and peroxodisulfuric acid ( $H_2S_2O_8$ ) was produced.  $H_2S_2O_8$  is a powerful oxidant ( $S_2O_8^{2-}/SO_4^{2-}$ ,  $E^\circ = 2.08$  V) able to achieve the oxidation of organic compounds; however, García-Gómez *et al.* (2014) reported that the presence of  $S_2O_8^{2-}$  does not influence the degradation of CBZ. Based on the results of the preliminary experiments, currents intensities of 1.2 and 3.0 A and oxygen flow of 1.5 and 3.0 L  $O_2$ /min were chosen for the experimental FD methodology in the present study. The ranges of the independent variables are shown in Table 2.

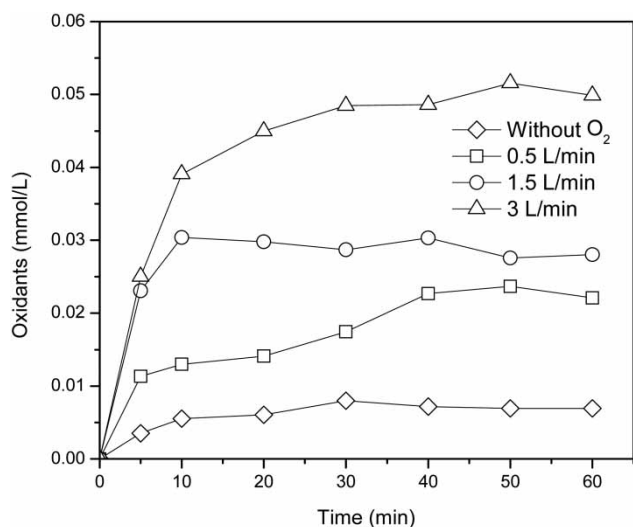


Figure 3 | Oxidants electrogenerated at different oxygen flux and 3.0 A.

Table 2 | Experimental range and levels of independent variables

Variable ( $X_i$ )	Factor ( $U_i$ )	Description	Experimental range	
			Min. value (-1)	Max. value (+1)
$X_1$	$U_1$	Time (min)	40	110
$X_2$	$U_2$	Current intensity (A)	1.2	3.0
$X_3$	$U_3$	pH	4	8
$X_4$	$U_4$	Oxygen flux (L/min)	1.5	3.0

## 2<sup>4</sup> FD

The experimental response for a 2<sup>4</sup> FD is represented by a linear polynomial model with interaction as follows:

$$Y = b_0 + b_1X_1 + b_2X_2 + b_3X_3 + b_4X_4 + b_{12}X_1X_2 + b_{13}X_1X_3 + b_{14}X_1X_4 + b_{23}X_2X_3 + b_{24}X_2X_4 + b_{34}X_3X_4$$

where  $Y$  represents the experimental response (CBZ or COD removal);  $b_0$  represents the average value of the responses of the 16 assays;  $X_i$  and  $X_j$  are the coded variable (-1 or +1);  $b_i$  represents the principal effect of each factor  $i$  on the response and  $b_{ij}$  represents the interaction effect between factor  $i$  and factor  $j$  on the response. The coefficients of the polynomial model were calculated by means of Design Expert<sup>®</sup> software (Table 3). The empirical relationship between the response and the variables are expressed by the following polynomial equations:

$$Y_{CBZ} = 62.23 + 9.69X_1 + 4.40X_2 + 1.01X_3 + 4.03X_4 + 1.09X_1X_2 + 0.49X_1X_3 - 0.39X_1X_4 + 0.50X_2X_3 + 0.16X_2X_4 + 0.66X_3X_4$$

$$Y_{COD} = 18.40 + 5.64X_1 + 4.47X_2 - 0.83X_3 + 0.22X_4 + 1.02X_1X_2 + 1.02X_1X_3 - 0.14X_1X_4 - 0.93X_2X_3 - 1.67X_2X_4 + 0.27X_3X_4$$

Coefficient of determination,  $R^2$ , is defined as the ratio of the explained variation to the total variation and is a measure of the degree of fit; for a good fit of a model,  $R^2$  should be at least 0.80 (Fu *et al.* 2007). The regression analysis with  $R^2$  value of 0.9793 for CBZ removal and 0.9276 for COD removal shows a close fit between the experimental results and the model predictions. The coefficient  $b_0$  indicates the average removal of the 16 assays (62.23% and 18.40% for CBZ and COD removal, respectively). The electrolysis time greatly influences with positive effect both rate removals ( $b_{1CBZ} = 9.69$ ,  $b_{1COD} = 5.64$ ). Thus, the percentage of CBZ degradation

**Table 3** | Experimental factorial matrix in the 2<sup>4</sup> FD and experimental results

	Experiment design				Experimental plan				Actual CBZ removal (%)	Predicted CBZ removal (%)	Actual COD removal (%)	Predicted COD removal (%)
	X <sub>1</sub>	X <sub>2</sub>	X <sub>3</sub>	X <sub>4</sub>	U <sub>1</sub> (min)	U <sub>2</sub> (A)	U <sub>3</sub>	U <sub>4</sub> (L/min)				
1	-1	-1	-1	-1	40	1.2	4	1.5	45.96	45.60	6.21	8.75
2	-1	+1	-1	-1	40	3.0	4	1.5	64.02	62.60	18.24	15.66
3	-1	-1	+1	-1	40	1.2	8	1.5	49.90	50.90	20.57	20.84
4	-1	+1	+1	-1	40	3.0	8	1.5	71.49	72.26	32.07	31.85
5	+1	-1	-1	-1	110	1.2	4	1.5	45.43	44.31	10.45	6.38
6	+1	+1	-1	-1	110	3.0	4	1.5	60.38	63.28	13.24	17.36
7	+1	-1	+1	-1	110	1.2	8	1.5	51.16	51.63	13.50	14.77
8	+1	+1	+1	-1	110	3.0	8	1.5	77.21	74.96	31.16	29.85
9	-1	-1	-1	+1	40	1.2	4	3.0	50.15	52.81	11.78	11.71
10	-1	+1	-1	+1	40	3.0	4	3.0	69.12	68.24	19.07	19.19
11	-1	-1	+1	+1	40	1.2	8	3.0	62.05	58.74	19.84	17.11
12	-1	+1	+1	+1	40	3.0	8	3.0	77.00	78.53	26.00	28.69
13	+1	-1	-1	+1	110	1.2	4	3.0	55.36	54.17	8.79	10.40
14	+1	+1	-1	+1	110	3.0	4	3.0	72.16	71.57	23.62	21.96
15	+1	-1	+1	+1	110	1.2	8	3.0	60.29	62.12	10.90	12.10
16	+1	+1	+1	+1	110	3.0	8	3.0	83.93	83.88	28.90	27.75

increases on average by 19.38% ( $2 \times 9.69$ ) when the reaction time goes from 40 to 110 min; meantime, the COD reduction increases 11.28% ( $2 \times 5.64$ ). The second most important factor for both removals is the current intensity with a positive effect ( $b_{2\text{CBZ}} = 4.40$ ,  $b_{2\text{COD}} = 4.47$ ). pH exerts a non-significant effect ( $b_{3\text{CBZ}} = 1.01$ ,  $b_{3\text{COD}} = -0.83$ ). This can be explained by the high  $pK_a$  value of CBZ (13.9), which means that this molecule does not suffer any appreciable dissociation along the whole pH interval. It is important to note that oxygen flux shows an important positive effect ( $b_{4\text{CBZ}} = 4.03$ ) in CBZ removal, indicating an increase of 8.06% ( $2 \times 4.03$ ) when the oxygen flux increases from 1.5 to 3.0 L/min.

However, based on the COD decrease, the effect of oxygen flux, meaning ROS production, was relatively weak ( $b_{4\text{COD}} = 0.22$ ). It seems that the oxidant power of the electro-generated species such as  $\text{H}_2\text{O}_2$  ( $E^\circ(\text{H}_2\text{O}_2/\text{H}_2\text{O}) = 1.77 \text{ V}$ ) is not enough for the COD decrease. Further, the low COD removal obtained (up to 31%) was due to the limited efficiency of the electrochemical oxidation of simple organic compounds (methanol, formic acid, etc.). In fact, only platinum-based electrodes can allow mineralization of the simple organic compounds (Comninellis & Chen 2010). In our case, methanol contributes 80% of the total COD. Similar results about the low COD removal were obtained by Wu et al. (2012), who removed the antibiotic tetracycline by

electrochemical process and achieved 33% COD removal efficiency after 480 min using Ti/RuO<sub>2</sub>-IrO<sub>2</sub> anode. However, Daghri et al. (2014) removed up to 78.2% of COD of domestic wastewater using Ti/BDD anode at 26.53 mA/cm<sup>2</sup> after 120 min of electrolysis, and Guitaya et al. (2014) reached a 70% removal in 90 min at 3.0 A treating domestic wastewater. Hence, the COD removal depends on the type of the organic compound and its affinity and interaction with oxidant species. Among the interaction terms, electrolysis time-current intensity ( $X_1X_2$ ) has the most important positive coefficient for CBZ removal ( $b_{12} = 1.09$ ). For COD decrease, the interactions electrolysis time-current intensity ( $X_1X_2$ ) and electrolysis time-pH ( $X_1X_3$ ) are the most important ( $b_{12} = 1.02$ ,  $b_{13} = 1.02$ ) with same positive effect. Pareto analysis calculates the percentage effect of each factor on the response; hence, this analysis may be used in order to get more significant information to interpret the results (Equation (7)).

$$P_i = \left( \frac{b_i^2}{\sum_{i=1}^k b_i^2} \right) * 100 \quad (i \neq 0) \quad (7)$$

where  $b_i$  represents the estimation of the main effect of the factor  $i$ . The contribution of the primary effects on the percentage of CBZ degradation are 70.7, 14.6, 0.8 and 12.3% for

electrolysis time, current intensity, initial pH and oxygen flux, respectively. For the same principal factors in the case of COD removal, the contributions are 54.5, 34.2, 1.18 and 0.08%. As shown in Figure 4, for both CBZ and COD removal, time is the factor with the higher contribution, followed by current intensity.

It is essential to note that the indirect oxidation by means of electrogenerated ROS has a significant contribution in the CBZ removal (12.3%). Nevertheless, the effect of indirect oxidation is negligible (0.08%) in COD

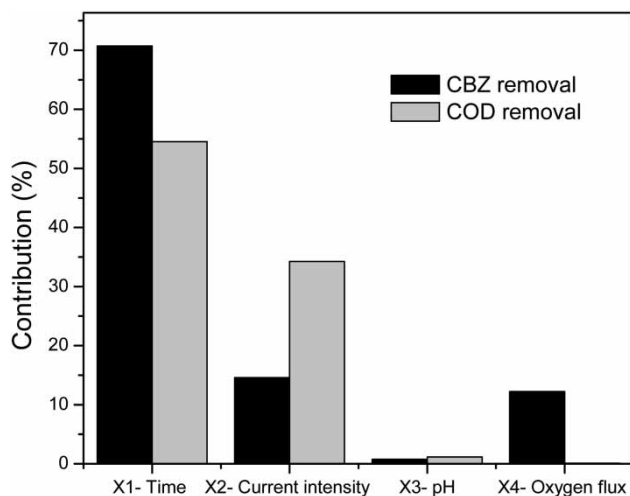


**Figure 4** | Graphical Pareto analysis of the effect of time, current intensity, pH and oxygen flux on CBZ and COD removal.

decrease. The contribution of the interaction effects ( $X_1X_2$ ,  $X_1X_3$ ,  $X_1X_4$ ,  $X_2X_3$ ,  $X_2X_4$  and  $X_3X_4$ ) (values omitted in Figure 4) on the percentage of CBZ degradation are the following: 0.9, 0.2, 0.1, 0.2, 0.02 and 0.3%, respectively. For COD decrease the contribution of the interaction effects are: 1.8, 1.8, 0.03, 1.5, 4.8 and 0.1%. From the FD it is clearly observed that the increase of treatment time, current intensity and oxygen flux enhances the amount of oxidant species produced and consequently increases the degradation efficiency of the pollutant. Once interactions affecting the response and the region of the optimum parameters have been determined, a more elaborated model, such as the second order model, may be employed. For this reason, a CCD should be used in a second step to determine the optimal operating conditions.

#### Optimization conditions for CBZ removal using central composite design methodology

The objective of RSM is to determine the optimum operating conditions for the system or to obtain a region in which operating requirements are satisfied. In our case, the RSM consists of a  $2^4$  factorial with 16 runs (described above), eight axial runs (assays 17–24) and six center runs (assays 25–30) (Table 4). The reason for including center runs is to provide reasonably stable variance of predicted response (Montgomery 2008). For the evaluation of data, the

**Table 4** | Central composite matrix, experimental and predicted results

Exp	Experiment design				Experimental plan				Actual CBZ removal (%)	Predicted CBZ removal (%)	Actual COD removal (%)	Predicted COD removal (%)
	$X_1$	$X_2$	$X_3$	$X_4$	$U_1$ (min)	$U_2$ (A)	$U_3$	$U_4$ (L/min)				
17	$-\alpha$	0	0	0	5	2.1	6	2.25	47.03	43.08	2.00	3.72
18	$+\alpha$	0	0	0	145	2.1	6	2.25	81.86	80.52	23.88	26.06
19	0	$-\alpha$	0	0	75	0.3	6	2.25	63.90	59.53	5.06	9.10
20	0	$+\alpha$	0	0	75	3.9	6	2.25	76.34	75.42	29.23	29.08
21	0	0	$-\alpha$	0	75	2.1	2	2.25	65.00	61.34	17.00	19.38
22	0	0	$+\alpha$	0	75	2.1	10	2.25	66.00	64.37	15.00	16.51
23	0	0	0	$-\alpha$	75	2.1	6	0.75	62.21	55.85	9.64	15.41
24	0	0	0	$+\alpha$	75	2.1	6	3.75	67.20	68.27	21.98	20.10
25	0	0	0	0	75	2.1	6	2.25	66.59	66.62	22.50	22.43
26	0	0	0	0	75	2.1	6	2.25	68.55	66.62	23.88	22.43
27	0	0	0	0	75	2.1	6	2.25	66.97	66.62	21.99	22.43
28	0	0	0	0	75	2.1	6	2.25	65.73	66.62	20.15	22.43
29	0	0	0	0	75	2.1	6	2.25	65.56	66.62	23.45	22.43
30	0	0	0	0	75	2.1	6	2.25	66.33	66.62	22.60	22.43

experimental response was described by a second order model in the form of a quadratic polynomial, given by the following equation:

$$Y = b_0 + \sum_{i=1}^k b_i X_i + \sum_{i=1}^k b_{ii} X_i^2 + \sum_j \sum_{i=2}^k b_{ij} X_i X_j + e_i$$

where  $Y$  is the experimental response;  $X_i$  and  $X_j$  are the independent variables;  $b_0$  is the average of the experimental response;  $b_i$  is the estimation of the principal effect of the factor  $j$  on the response  $Y$ ;  $b_{ii}$  is the estimation of the second effect of the factor  $i$  on the response  $Y$ ;  $b_{ij}$  is the estimation of the interaction effect between  $i$  and  $j$  on the response  $Y$  and  $e_i$  represents the error on the response  $Y$ . Based on the results, the coefficients of the quadratic model were calculated using the Design Expert® software:

$$Y_{CBZ} = 19.279048 + 0.33881X_1 - 1.49418X_2 + 1.0943452X_3 + 5.621746X_4 + 0.034623X_1X_2 + 0.00702X_1X_3 - 0.00748X_1X_4 + 0.2802X_2X_3 + 0.1162X_3X_4 - 0.0009X_1^2 + 0.2635X_2^2 - 0.2354X_3^2 - 0.5068X_4^2$$

$$Y_{COD} = -39.55194 + 0.22247X_1 + 16.10231X_2 + 2.59098X_3 + 7.31742X_4 + 0.03250X_1X_2 + 0.01455X_1X_3 + 0.0027X_1X_4 - 0.51458X_2X_3 - 1.2398X_2X_4 + 0.0887X_3X_4 - 0.0015X_1^2 - 1.0293X_2^2 - 0.2800X_3^2 - 0.5188X_4^2$$

The predicted 3D surface plots for CBZ removal are shown in Figure 5. When the oxygen flux and pH were kept constant (at 2.8 L/min and 7.0, respectively), CBZ removal efficiency enhanced with increasing current intensity and electrolysis time throughout the interval studied (Figure 5(a)). Similar behavior is shown in Figure 5(b); at 110 min and oxygen flux of 2.8 L/min, CBZ removal increased as a function of current intensity and pH.

Table 5 shows the analysis of variance (ANOVA) of regression parameters of the predicted response surface quadratic model for CBZ and COD removal using electrooxidation and *in situ* ROS production process. As can be seen from this table, the model F-value of 15.81 for CBZ removal and 9.42 for COD removal, and a low probability value in both processes ( $Pr > F = 0.0001$ ), indicate that the lack of fit of the model is not significant for both CBZ and COD removal.

Moreover, the value of the correlation coefficient ( $R_{CBZ}^2 = 0.9365$ ,  $R_{COD}^2 = 0.8979$ ) indicates that only 6.35 and 10.21% of the total variation for each removal could not be explained by the empirical model. Hence, the agreement between actual and predicted values of CBZ degradation and COD removal is satisfactory and consistent with the quadratic model. The target of the optimization is to determine the optimum values for both CBZ and COD removal. The criteria selected for the optimization condition are the following: (I) CBZ and COD removal have to be maximized; (II) the four variables have to be investigated throughout the experimental range; (III) because the CBZ removal is the main objective of the present investigation,

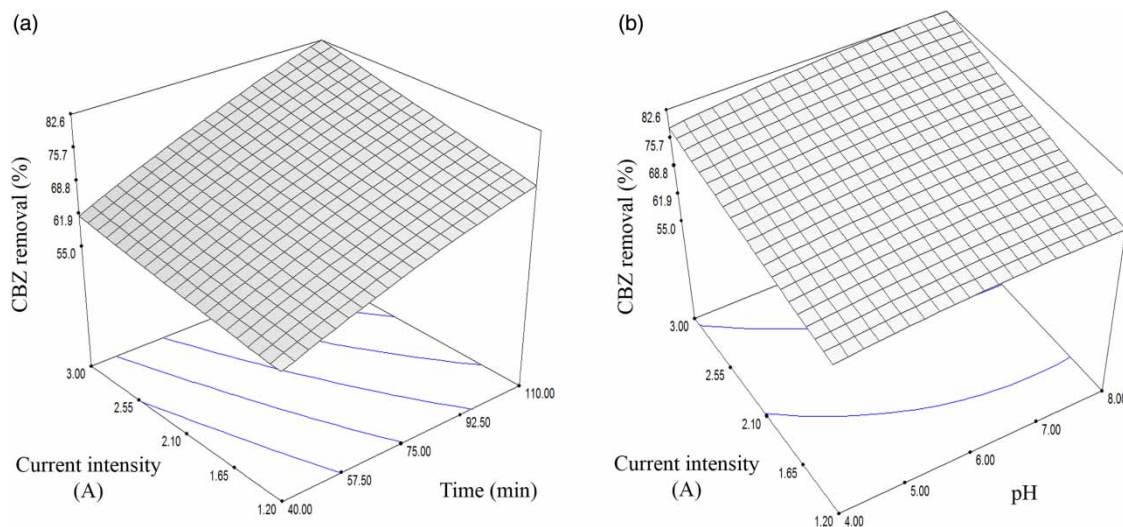


Figure 5 | CBZ degradation as a function of (a) electrolysis time and current intensity; (b) pH and current intensity: three-dimensional plot obtained from central composite matrix.

**Table 5** | ANOVA results for the response surface quadratic model for CBZ and COD removal

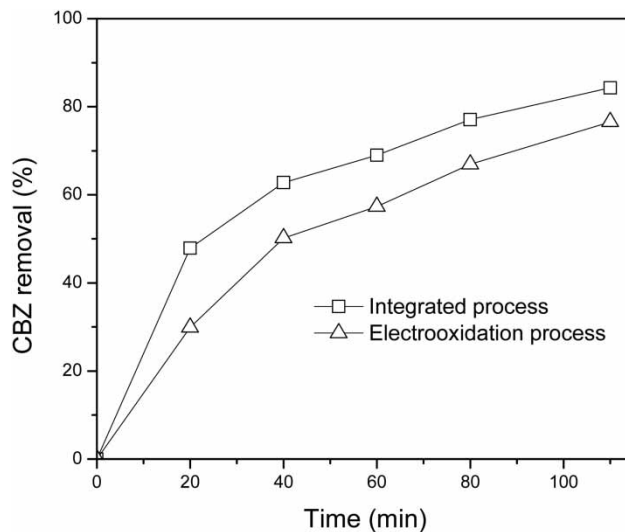
ANOVA					
	d.f. <sup>a</sup>	Sum of square	Mean of square	F-value	Pr > F
CBZ removal					
Model	14	2851.46	203.68	15.81	<0.0001
Residual	15	193.23	12.88		
Lack of fit	10	187.39	18.74	16.02	0.0034
Pure error	5	5.85	1.17		
COD removal					
Model	14	1625.44	116.1	9.42	<0.0001
Residual	15	184.85	12.32		
Lack of fit	10	176.28	17.63	10.29	0.0095
Pure error	5	8.57	1.71		

F = Fisher coefficient.

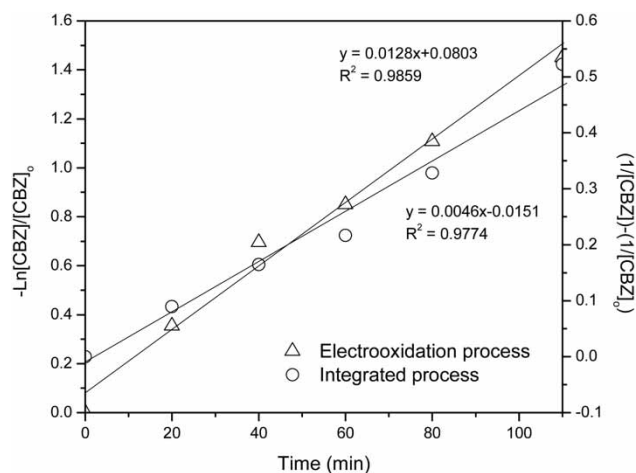
<sup>a</sup>Degrees of freedom. $R^2$  for CBZ removal = 0.9365. $R^2$  for COD removal = 0.8979.

its concentration has to be minimized with the highest importance (5/5 weighting factor) and COD removal has to be increased with lesser importance (3/5 weighting factor). Based on the criteria mentioned before, the best operating conditions proposed by Design Expert<sup>®</sup> software are the following: 110 min of electrolysis at 3.0 A, pH = 7.05 and 2.8 L O<sub>2</sub>/min. Under these optimal conditions the theoretical response proposed by the software was: 82.44 and 29.99% for CBZ and COD removal, respectively, with desirability of 0.945. To confirm the model reproducibility and the validity of the optimization procedure, a set of three additional experiments was performed under optimal operating conditions. After, in order to evaluate the effect of the indirect oxidation, assays were performed in the optimal conditions in the absence of oxygen added.

Figure 6 shows the CBZ removal through time in optimal conditions. It shows a rapid oxidation of the compound, followed by a slow attenuation rate after 40 min of electrolysis. During 110 min of treated time in the optimal conditions, the model prediction (82.44% for CBZ removal and 29.99% for COD removal) fits very well with the yield experimentally obtained (83.90% ± 0.8% and 32.38% ± 1.0%, respectively). In order to evaluate the oxidation rate of CBZ, the kinetic data were analyzed using first and second order kinetic models under the optimum conditions. The model with the higher correlation coefficient ( $R^2$ ) was chosen as the appropriate one for the process. The best fitting model for the electrooxidation and *in situ* ROS production was the

**Figure 6** | Removal of CBZ using optimal conditions by means of the integrated process and electrooxidation process (in the absence of oxygen added).

second order with  $R^2$  of 0.9774 and an apparent rate constant for oxidative removal of CBZ of 0.0046 M<sup>-1</sup>s<sup>-1</sup>. In the absence of oxygen (without ROS production) the CBZ removal was 76.56% and COD decrease was 30.75%; the apparent rate constant was 0.0128 min<sup>-1</sup> ( $t_{1/2}$  = 54.15 min) fitting in the first order reaction kinetic ( $R^2$  = 0.9859) (Figure 7). It is interesting to compare the kinetic constant with values obtained in others experimental conditions. Dagherir *et al.* (2013) indicated that the degradation kinetic of CBZ using the photoelectrocatalytic process at Ti/TiO<sub>2</sub> nanostructured electrodes is well described by the pseudo-second order kinetic model with a kinetic rate constant of 6 × 10<sup>-4</sup> L mg<sup>-1</sup> min<sup>-1</sup>. However, the first order kinetic

**Figure 7** | Degradation kinetics of CBZ removal by means of the integrated process and electrooxidation process (in the absence of oxygen added).

model for CBZ removal using an electrochemical process was obtained in other works. Palo *et al.* (2014) tested electrodegradation of CBZ in various aqueous matrices and presented a first order reaction rate constant of 0.73, 0.20 and 0.55 min<sup>-1</sup>, for distilled water, wastewater and surface water, respectively. García-Gómez *et al.* (2014) investigated the CBZ electrooxidation using Ti/BDD and Ti/PbO<sub>2</sub> anodes, and obtained a removal rate constant of 0.021 min<sup>-1</sup>. It is important to note that the *in situ* ROS production modifies the kinetic order due to the participation of other reactives in the removal reaction.

Even though the present work shows significant information about the removal of the recalcitrant compound CBZ by means of an integrated process using electrochemical direct oxidation and *in situ* ROS production indirect oxidation, the next step is to use a more specific analytic technique for quantification of the compound concentration, such as liquid chromatography mass spectrometry. Furthermore, by-products need to be identified and the reaction pathways for CBZ degradation might be proposed.

## CONCLUSIONS

The degradation of CBZ was carried out applying an integrated process of electrooxidation and *in situ* ROS production in an electrochemical reactor with Ti/PbO<sub>2</sub> anode located between Ti cylindrical mesh cathodes.

From a complete 2<sup>4</sup> FD, electrolysis time, current intensity and oxygen flux were found to be the most important variables for the CBZ removal and pH exerts a non-significant effect (70.7%, 14.6%, 12.3% and 0.8%, respectively).

A CCD was employed to define the optimal operating conditions. Based on the criteria selected, the best operating conditions proposed by Design Expert<sup>®</sup> software are the following: 110 min of electrolysis at 3.0 A, pH = 7.05 and 2.8 L O<sub>2</sub>/min. Under these optimal conditions the experimental response for CBZ removal (83.90 ± 0.8%) fits very well with the model prediction (82.44%). Both FD and CCD models presented correlation factors above 0.89.

Up to 0.05 mmol/L of ROS was produced at 3.0 L O<sub>2</sub>/min; however, indirect oxidation does not present significant effect (0.08%) for COD removal.

The kinetic study shows that the second order kinetic model accurately describes the oxidation of CBZ by means of the electrooxidation and *in situ* ROS production process.

The proposed integrated process is a promising technology for recalcitrant compounds removal in wastewater.

## ACKNOWLEDGEMENTS

The authors are grateful to the Mexican Institute of Water Technology (IMTA) and the National Council of Science and Technology (CONACyT) for their financial support to this study.

## REFERENCES

- Al Aukidy, M., Verlicchi, P., Jelic, A., Petrovic, M. & Barcelo, D. 2012 Monitoring release of pharmaceutical compounds: occurrence and environmental risk assessment of two WWTP effluents and their receiving bodies in the Po Valley, Italy. *Science of the Total Environment* **438**, 15–25.
- Chenxi, W., Spongberg, A. L. & Witter, J. D. 2008 Determination of the persistence of pharmaceuticals in biosolids using liquid-chromatography tandem mass spectrometry. *Chemosphere* **73** (4), 511–518.
- Comninellis, C. & Chen, G. 2010 *Electrochemistry for the Environment*. Springer, New York.
- Comninellis, C., Kapalka, A., Malato, S., Parsons, S. A., Poullos, I. & Mantzavinos, D. 2008 Advanced oxidation processes for water treatment: advances and trends for R&D. *Journal of Chemical Technology & Biotechnology* **83** (6), 769–776.
- Daghrir, R., Drogui, P., Dimboukou-Mpira, A. & El Khakani, M. A. 2013 Photoelectrocatalytic degradation of carbamazepine using Ti/TiO<sub>2</sub> nanostructured electrodes deposited by means of a pulsed laser deposition process. *Chemosphere* **93** (11), 2756–2766.
- Daghrir, R., Drogui, P. & Tshibangu, J. 2014 Efficient treatment of domestic wastewater by electrochemical oxidation process using bored doped diamond anode. *Separation and Purification Technology* **131**, 79–83.
- Dai, Q., Xia, Y., Sun, C., Weng, M., Chen, J., Wang, J. & Chen, J. 2014 Electrochemical degradation of levodopa with modified PbO<sub>2</sub> electrode: parameter optimization and degradation mechanism. *Chemical Engineering Journal* **245**, 359–366.
- Fu, J., Zhao, Y. & Wu, Q. 2007 Optimising photoelectrocatalytic oxidation of fulvic acid using response surface methodology. *Journal of Hazardous Materials* **144** (1–2), 499–505.
- García-Gómez, C., Drogui, P., Zavisca, F., Seyhi, B., Gortáres-Moroyoqui, P., Buelna, G., Neira-Sáenz, C., Estrada-alvarado, M. & Ulloa-Mercado, R. G. 2014 Experimental design methodology applied to electrochemical oxidation of carbamazepine using Ti/PbO<sub>2</sub> and Ti/BDD electrodes. *Journal of Electroanalytical Chemistry* **732**, 1–10.
- Guitaya, L., Drogui, P. & Blais, J. F. 2014 In situ reactive oxygen species production for tertiary wastewater treatment. *Environmental Science and Pollution Research*. **22** (9), 7025–7036.
- Jiang, W., Joens, J., Dionysiou, D. & O'Shea, K. 2013 Optimization of photocatalytic performance of TiO<sub>2</sub> coated glass microspheres using response surface methodology and the application for degradation of dimethyl phthalate. *Journal of Photochemistry and Photobiology A: Chemistry*. **262**, 7–13.

- Khataee, A. R., Safarpour, M., Zarei, M. & Aber, S. 2011 Electrochemical generation of H<sub>2</sub>O<sub>2</sub> using immobilized carbon nanotubes on graphite electrode fed with air: investigation of operational parameters. *Journal of Electroanalytical Chemistry* **659** (1), 63–68.
- Miao, X.-S., Yang, J.-J. & Metcalfe, C. D. 2005 Carbamazepine and its metabolites in wastewater and in biosolids in a municipal wastewater treatment plant. *Environmental Science & Technology* **39** (19), 7469–7475.
- Mohapatra, D. P., Brar, S. K., Tyagi, R. D., Picard, P. & Surampalli, R. Y. 2014a Analysis and advanced oxidation treatment of a persistent pharmaceutical compound in wastewater and wastewater sludge-carbamazepine. *Science of the Total Environment* **470–471**, 58–75.
- Mohapatra, D. P., Brar, S. K., Daghrir, R., Tyagi, R. D., Picard, P., Surampalli, R. Y. & Drogui, P. 2014b Photocatalytic degradation of carbamazepine in wastewater by using a new class of whey-stabilized nanocrystalline TiO<sub>2</sub> and ZnO. *Science of The Total Environment* **485–486**, 263–269.
- Monsalvo, V. M., Lopez, J., Munoz, M., de Pedro, Z. M., Casas, J. A., Mohedano, A. F. & Rodriguez, J. J. 2015 Application of Fenton-like oxidation as pre-treatment for carbamazepine biodegradation. *Chemical Engineering Journal* **264**, 856–862.
- Montgomery, D. C. 2008 *Design and Analysis of Experiments*. Wiley, New York.
- Palo, P., Domínguez, J. R. & Sánchez-Martín, J. 2012 Ozonation of a carbamazepine effluent. Designing the operational parameters under economic considerations. *Water, Air, & Soil Pollution* **223** (9), 5999–6007.
- Palo, P., Dominguez, J. R., Gonzalez, T., Sanchez-Martin, J. & Cuerda-Correa, E. M. 2014 Feasibility of electrochemical degradation of pharmaceutical pollutants in different aqueous matrices: optimization through design of experiments. *Journal of Environmental Science and Health A* **49** (7), 843–850.
- Peralta, E., Natividad, R., Roa, G., Marin, R., Romero, R. & Pavan, T. 2013 A comparative study on the electrochemical production of H<sub>2</sub>O<sub>2</sub> between BDD and graphite cathodes. *Sustainable Environment Research* **23** (4), 259–266.
- Shen, Z., Yang, J., Hu, X., Lei, Y., Ji, X., Jia, J. & Wang, W. 2005 Dual electrodes oxidation of dye wastewater with gas diffusion cathode. *Environmental Science & Technology* **39** (6), 1819–1826.
- Tran, L.-H., Drogui, P., Mercier, G. & Blais, J.-F. 2009 Electrolytic oxidation of polynuclear aromatic hydrocarbons from creosote solution using Ti/IrO<sub>2</sub> and Ti/SnO<sub>2</sub> circular mesh electrodes. *Journal of Environmental Engineering* **135** (10), 1051–1062.
- Tran, N. & Drogui, P. 2013 Electrochemical removal of microcystin-LR from aqueous solution in the presence of natural organic pollutants. *Journal of Environmental Management* **114**, 253–260.
- Tran, N., Drogui, P., Zaviscka, F. & Brar, S. K. 2013 Sonochemical degradation of the persistent pharmaceutical carbamazepine. *Journal of Environmental Management* **131**, 25–32.
- Wu, J., Zhang, H., Oturan, N., Wang, Y., Chen, L. & Oturan, M. A. 2012 Application of response surface methodology to the removal of the antibiotic tetracycline by electrochemical process using carbon-felt cathode and DSA (Ti/RuO<sub>2</sub>-IrO<sub>2</sub>) anode. *Chemosphere* **87** (6), 614–620.
- Yang, K. S., Mul, G. & Mouljn, J. A. 2007 Electrochemical generation of hydrogen peroxide using surface area-enhanced Ti-mesh electrodes. *Electrochimica Acta* **52** (22), 6304–6309.
- Zhang, Y., Geissen, S. U. & Gal, C. 2008 Carbamazepine and diclofenac: removal in wastewater treatment plants and occurrence in water bodies. *Chemosphere* **73** (8), 1151–1161.
- Zhu, H., Chen, Y., Qin, T., Wang, L., Tang, Y., Sun, Y. & Wan, P. 2014 Lignin depolymerization via an integrated approach of anode oxidation and electro-generated H<sub>2</sub>O<sub>2</sub> oxidation. *RSC Advances* **4** (12), 6232–6238.

First received 7 July 2015; accepted in revised form 5 November 2015. Available online 19 November 2015